Terahertz (Far-Infrared) Characterization of Tris(hydroxymethyl)aminomethane Using High-Resolution Waveguide THz-TDS

S. Sree Harsha and D. Grischkowsky*

School of Electrical and Computer Engineering, Oklahoma State University, Stillwater, Oklahoma 74078

Received: November 23, 2009; Revised Manuscript Received: February 1, 2010

Waveguide THz-TDS using metal parallel plate waveguides is employed to obtain a high-resolution terahertz vibrational spectrum of tris(hydroxymethyl)aminomethane, commonly known as Tris or THAM, an important biological buffer component, a neuroinhibitor and an organic thermal energy-storing molecule. Dropcast and sublimated thin films are used to characterize the sample. The development (with cooling) of 3 broad resonances seen at room temperature into 12 highly resolved spectral features for the dropcast sample and 11 features for a sublimated sample at 13.6 K is tracked by measuring the temperature dependence of the transmission spectrum. Resonances with fwhm linewidths as narrow as 12 GHz are obtained. These results provide strong constraints on theoretical modeling.

Introduction

Tris(hydroxymethyl)aminomethane (Tris) is an amino alcohol extensively used in biochemistry and molecular biology as a component of buffer solutions since its first introduction by Gomori in 1946.[1,2] Commonly known as Tris or THAM, it is a stable white crystalline powder having high solubility in water. Since its first use as a buffer component, this molecule has proven to have other important applications, such as in the field of medicine as well as in thermal energy storage.[3,4]

Tris is used as a component of buffer solutions, such as in TAE (Tris−acetate−EDTA) and TBE (Tris−borate−EDTA) buffer, especially for solutions of nucleic acids. Tris has a pK_a of 8.06, which implies that the buffer has an effective pH range of 7−9. The useful buffer range for Tris of 7−9 coincides with the typical physiological pH of most living organisms.[1,2] This and its low cost make Tris one of the most important buffers used in biology and biochemistry.[5−8] This widely used buffering agent has also been shown to act as an inhibitor of acetocholine, a neurotransmitter found in both the peripheral nervous system and the central nervous system in many organisms, including humans. At concentrations ranging from 5 to 10 mM, it has been demonstrated to function as a potent inhibitor of both excitatory and inhibitory responses to iontophoretically applied acetylcholine.[9,10] More recently, Tris has been used in the field of medicine as a drug to cure metabolic acidosis in acute lung injury.[3,4,11]

Tris is known to exist in two phases, a crystalline phase and a plastic phase, undergoing a solid−solid phase transition at 407.3 °C from a crystalline orthorhombic lattice to an orientationally disordered body centered cubic lattice.[10,12] The molecule undergoes a large change in enthalpies at the transition from orientationally ordered to disordered plastic phases. Due to the presence of the enthalpy changes, Tris has been used as an organic thermal energy storage material having applications in solar cell systems.[13]

To understand the function of Tris in these various roles, it is necessary to understand its molecular structure as well as the structural changes the molecule undergoes in the crystalline lattice under external influences. The far-infrared terahertz region from 0.1 to 10 THz (3 mm−30 μm, 3.33−333 cm^{-1}) has been shown to contain a wealth of information regarding low-frequency vibrational motion of molecules, both inter- and intramolecular. Consequently, by studying the vibrational spectra of molecules, it is often possible to understand the crystalline structure of the molecule and also to monitor the changes it undergoes by monitoring a change in its vibrational spectra. The vibrational mode frequencies give information about hydrogen bonding, conformational changes, effects of hydration, neighbor effects, and more. Raman and infrared studies of Tris have been reported in the literature,[14−16] but no terahertz (far-infrared) characterizations have so far been performed.

Another reason one needs to characterize this molecule is that it is a common buffer used for stabilizing the pH of many biological samples. It therefore becomes essential to know the complete vibrational spectrum of Tris to avoid erroneous assignment of some of the vibrational features of Tris to that of the biological sample being analyzed. The vibrational spectrum of molecules in aqueous solutions is often different as compared to the solid state crystalline films. Biological samples are studied in both the aqueous condition and solid state films. Knowing the complete vibrational spectrum of the buffer will be useful to determine the accurate vibrational response of the biological molecule.

In this paper, Tris is characterized in the terahertz range using the standard pellet technique and the newly developed high-resolution waveguide THz-TDS technique[17−19] to obtain an informative, high-resolution terahertz vibrational spectrum of the molecule. Waveguide THz-TDS using a metal parallel plate waveguide (PPWG) has been developed as a new spectroscopic tool to obtain high-resolution terahertz absorption spectra of materials using microgram sample quantities. Waveguide THz-TDS greatly complements standard THz-TDS[20,21] and far-infrared Fourier transform spectroscopy, and these techniques together can be used to completely characterize a material at terahertz frequencies.

Experimental Setup

The characterization of the sample was performed using a standard THz-TDS setup with high dynamic range illustrated

* E-mail: daniel.grischkowsky@okstate.edu.

10.1021/jp911135u
Published on Web 02/17/2010

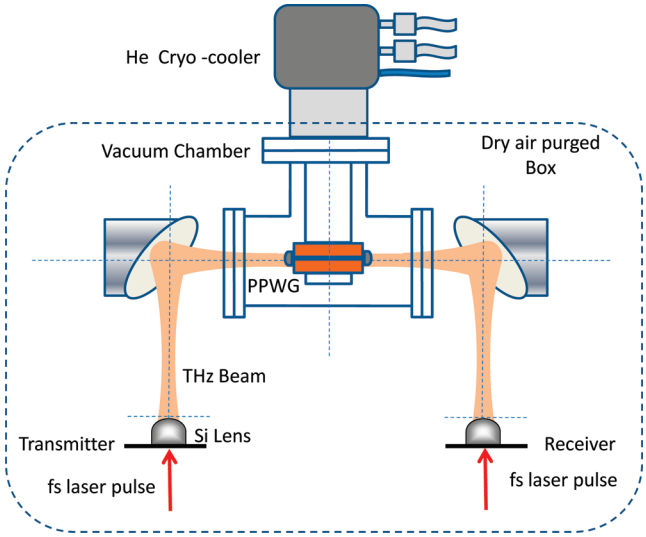

Figure 1. Apparatus for waveguide terahertz-TDS.

in Figure 1.[20,21] Terahertz radiation is generated and detected using photoconductive switches driven by 10 mW optical pulse trains from a 850 nm, 80 fs, 100 MHz mode locked Ti:sapphire femtosecond laser. The emitted terahertz radiation is collimated by a high-resistivity Si lens and a parabolic mirror. A measurement with a frequency resolution of 1 GHz and time domain signal-to-noise (S/N) ratio of 10 000 can be achieved with this system. The high dynamic range is desirable because the terahertz radiation is made to propagate through coupling optics for the PPWG and Si windows of the vacuum chamber, which attenuate the terahertz beam power. The entire system is located in an airtight enclosure to overcome the effects of water vapor absorption on the terahertz beams.

The PPWGs used for waveguide THz-TDS in this study were fabricated from aluminum, using standard machining tolerances. The dimensions of the two metal plates are 27.9 mm (width) × 30.5 mm (length) × 9.5 mm (thickness). The inner surfaces were polished to a mirror finish. The PPWG assembly with a 50 μm gap was obtained by placing four metal spacers at the corners of each of the plates. Terahertz pulses are coupled into and out of the PPWG using planocylindrical high-resistivity Si lenses at the entrance and exit faces of the PPWG assembly. The lenses are 15 mm (height) × 10 mm (width) × 6.56 mm (thickness), with a 5 mm radius of curvature. The PPWG was operated in the TEM mode as it exhibits nondispersive and low-loss terahertz pulse propagation.[22] The polarization of the terahertz field is perpendicular to the waveguide surface. Typical amplitude transmission efficiency through the 50 μm gap PPWG is in the range of 20−25% for frequencies near 1 THz without the cryocooler assembly. This includes coupling losses, losses due to the finite conductivity of the metal, and Fresnel reflections from the Si lenses. For experiments at low temperature, the waveguide assembly is placed inside a vacuum chamber with straight-through optical access and is mechanically attached to the coldfinger of a two-stage He cryocooler, as shown in Figure 1. With the cryocooler assembly in place, the total coupling efficiency is reduced by about a factor of 2 due to Fresnel reflections from the Si windows at the entrance and exit ports.

The instrumental spectral resolution is determined by the maximum temporal scan length, limited by reflections from the 6.56-mm-thick planocylindrical Si coupling lenses of the PPWG or the internal reflections of the 2 mm pellet for pellet measurements. For the pellet measurements, scan lengths of 33 ps were used. Scan lengths of 130 ps were used for the waveguide measurements, corresponding to a limiting resolution of 7.7 GHz. The time constant on the lockin amplifier was set at 100 ms with a 400 ms delay for each data point collected in the time domain. The total time taken for each temporal scan consisting of 2000 data points was 20 min. An average of four such scans was used to improve the S/N. All scans were zero-padded by approximately five times before taking the fast Fourier transform to obtain the spectral amplitude.[23]

Tris (99% pure) in white crystalline powder form was purchased from Sigma Aldrich and was used without further purification. Tris pellets were made by mixing 330 mg of polyethylene powder with 20 mg of Tris, and the mixture was pressed into pellets of thickness 2 mm and diameter 1 cm using a Carver hydraulic press. The sample powder was first finely ground using a mortar and pestle and then uniformly mixed with the polyethylene powder. This mixture was then poured into a die that had been preheated to ∼60 °C and then was pressed into a pellet by applying ∼11 tons of pressure. For the films used within the PPWG, the inner surface of the waveguide plate was first cleansed with solvent and then plasma-cleaned before casting the films. Two different film preparation techniques—namely, dropcasting and sublimation—were employed to get different microcrystal morphologies on the waveguide plates. Dropcasting from a solution of the sample gave macroscopic crystals, whereas sublimation yielded a uniform film with very small microcrystals.

The dropcast film was made by placing ∼200 μL of Tris solution in water (10 mg/mL) on the polished inner surface of the Al waveguide plate. The solution was allowed to evaporate overnight to obtain a planar distribution of fairly large microcrystals on the waveguide plate. Following evaporation, the relatively thick areas of the film along the outer edges were removed using a solvent soaked swab to leave a visually uniform film. Alternatively, ∼100−200 μg of the sample was placed in a glass sublimation unit, with the waveguide plate attached to the coldfinger. The unit was then evacuated and then heated to deposit a uniform film of Tris on the waveguide plate. Similar to the dropcast film, the outer edges were swabbed to obtain a rectangular patch of uniform film. This method yielded very small sized microcrystals, in comparison to the dropcast technique. The optical micrographs of both films are shown in Figure 2. A typical film mass was estimated to be ∼60−80 μg.

The waveguide plates were then bolted together with 50 μm spacers in between to form the metal PPWG. The planocylindrical Si lenses were attached onto the input and exit faces of the PPWG using custom-made lens holders. The terahertz absorption spectra of the Tris film were measured in this configuration from room temperature to 13.6 K. The sample temperature was measured by a Si diode temperature sensor attached to the waveguide. The variation of the absorption spectra with temperature was tracked by taking data at various intermediate temperatures. To extract the absorbance, a reference, A_{ref}, was estimated by fitting the amplitude spectra, A_{spec}, at points away from any sharp features with a spline. The amplitude absorbance was then calculated via the expression: Absorbance $= -\ln[A_{spec}/A_{ref}]$.

Results and discussion

Figure 3 shows the amplitude spectrum transmitted through the Tris−PE pellet at 13 K. The transmission through the pellet had spectral components all the way up to 4 THz. The transmission spectra at room temperature showed the presence of four absorption features at 1.23, 1.45, 1.75, and 2.11 THz. At 13 K, these features showed minimal narrowing and

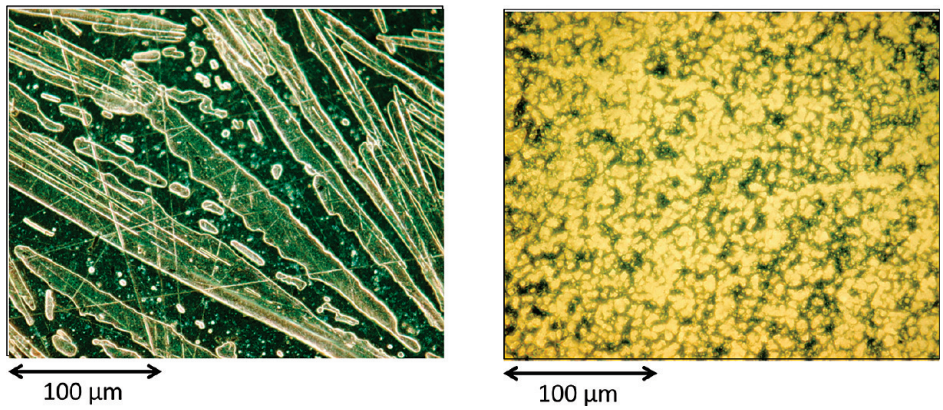

Figure 2. Optical micrographs of the Tris dropcast film on the left panel and the sublimated film on the right panel.

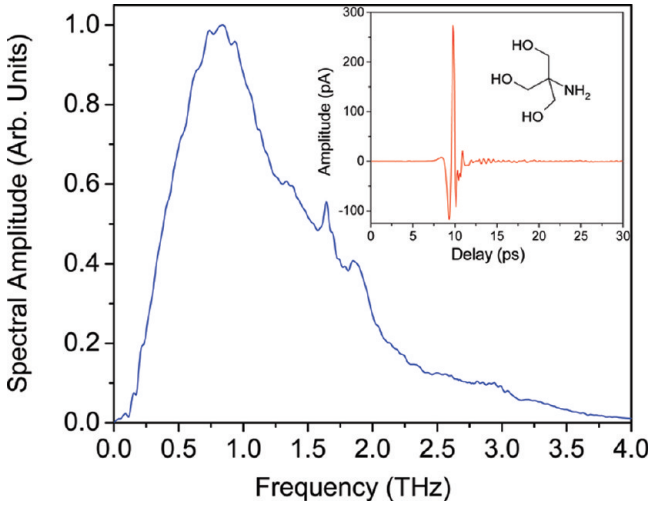

Figure 3. Output terahertz amplitude spectrum of Tris pellet at 13 K. Inset: Time domain trace of the terahertz pulse through the Tris pellet at 13 K.

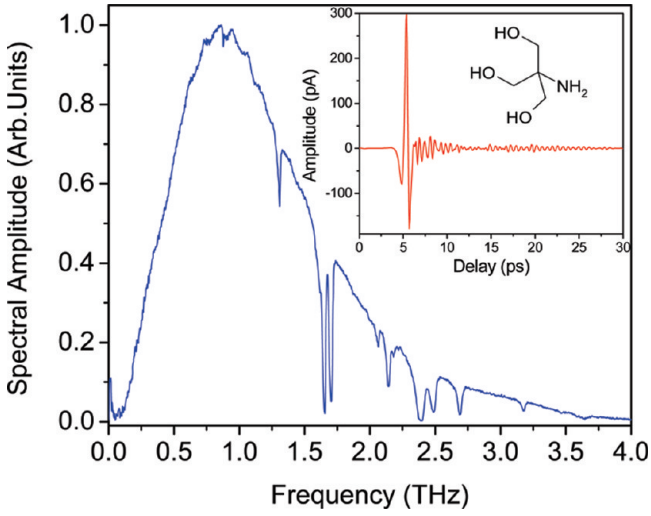

Figure 4. Output terahertz amplitude spectrum of dropcast Tris film within an aluminum PPWG at 13.6 K. Inset: Time domain trace of the terahertz pulse through the Tris waveguide at 13.6 K.

developed into features at 1.31, 1.57, 1.76, and 3.14 THz. The narrowest feature at 13 K had a fwhm of 150 GHz for the 1.76 THz line.

Figure 4 shows the amplitude spectrum transmitted through the dropcast film of Tris in the waveguide at 13.6 K. The temporal data shown in the inset exhibits a long ringing tail formed by the interference of various vibrational mode frequencies of the sample. The oscillations extend to almost 130 ps and are indicative of sharp resonances in the frequency domain. The transmission through the waveguide had spectral components extending all the way up to 4 THz, as shown in Figure 4. The transmission spectra at room temperature showed the presence of three absorption features at 1.5, 1.78, and 2.22 THz. In contrast to the pellets, upon cooling the waveguide film to 13.6 K, various thermal broadening mechanisms were quenched, and the transmission spectra evolved to reveal 12 highly resolved and narrow resonance features, as shown in Figure 4.

The snapshot of the thermal evolution of the amplitude spectra of the transmitted terahertz through the waveguide with dropcast film and the corresponding absorbance is shown in Figure 5. The thermal evolution shows the narrowing and splitting of resonances as the waveguide temperature reaches 13 K. The thermal evolution of transmission through a sublimated film waveguide and the corresponding absorbance is also shown in Figure 6. The waveguide with the sublimated film also showed three lines at 295 K at 1.51, 1.80, and 2.14 THz, which is similar to what was seen with a dropcast film, but upon cooling, the sublimated film shows a different evolution of the spectral features, which is indicative of the subtle changes in the crystal size and orientation between the two film preparation techniques. Upon cooling, the three spectral features of the sublimated film evolve into 11 narrow, well-resolved spectral features.

The spectral data, including line frequencies and line widths, derived either by performing nonlinear least-squares fits of the absorbance spectra or by direct estimation, for the pellet and both the films are collected and compared in Table 1.

Figure 7 compares the absorbance spectra at 13.6 K for sublimated and dropcast films and clearly shows the difference in evolution of spectral features for both the films with temperature. The sublimated film does not show resonances at 1.308, 2.064, 2.489, and 3.640 THz. The features at 2.173, 2.392, and 2.712 THz with linewidths 39, 25, and 39 GHz are broader than the corresponding features seen with dropcast film at 2.142, 2.393, and 2.691 THz with linewidths 27, 39, and 27 GHz, but the sublimated film shows three features that do not show up in the dropcast film: namely, at 1.629, the broad feature at 1.92, and 3.471 THz. At 13.6 K, the cluster of lines around 1.65 THz resolves into only two features at 1.655 and 1.706 THz with linewidths of 17 and 23 GHz in the dropcast film, whereas in the sublimated film, the cluster resolves into three features at 1.629, 1.647, and 1.70 THz with linewidths of 15, 12, and 20 GHz, respectively. The line at 1.647 THz is the narrowest,

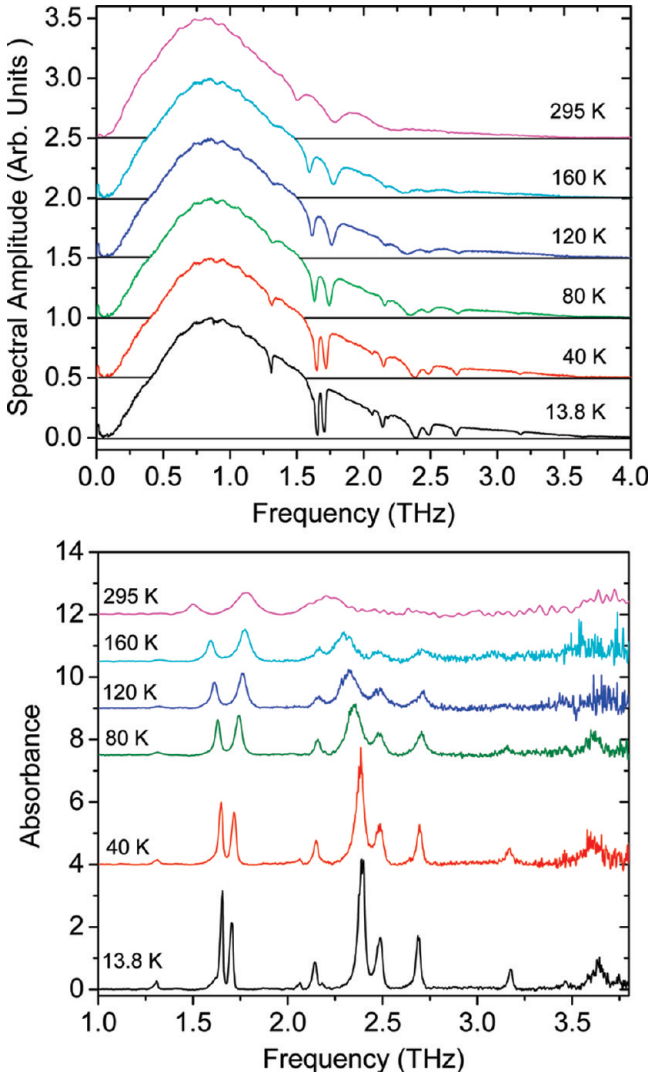

Figure 5. Spectral amplitudes (top panel) and absorbances (bottom panel) as a function of temperature for dropcast Tris thin films within polished aluminum PPWG. For clarity, the spectral amplitudes and absorbances from 40 to 295 K are offset.

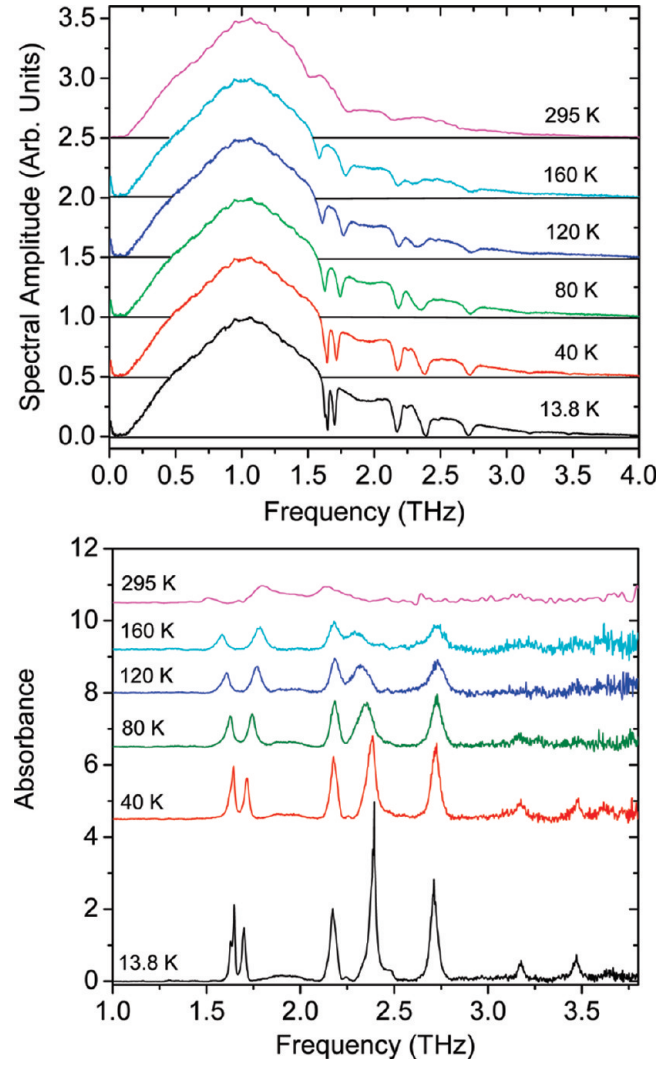

Figure 6. Spectral amplitudes (top panel) and absorbances (bottom panel) as a function of temperature for sublimated Tris thin films in polished aluminum PPWG. For clarity, the spectral amplitudes and absorbances from 40 to 295 K are offset.

having a fwhm of 12 GHz. The line at 2.484 THz in the sublimated film is very weak as compared to its dropcast counterpart.

Sublimated films are composed of microcrystals that are much smaller than the ones obtained by dropcast, as evident from Figure 2. There is a possibility that when the thin films of Tris are formed by the two different methods, the microcrystals may be oriented differently in the two films, and consequently, some of these modes, such as 1.308 and 2.484 THz in the sublimated film, may be diminished or totally absent due to the polarization dependence of the modes with respect to the propagating terahertz field.

A likely explanation for the narrower line shapes and more pronounced temperature dependence of the waveguide films is that the vibrational modes of the film contain a smaller degree of inhomogeneous broadening than do those of traditional pellet samples. Vibrational line shapes for molecular solids typically display a mixture of homogeneous (dynamic) and inhomogeneous (static) broadening. Homogeneous broadening mechanisms, such as vibrational energy exchange and pure dephasing, are temperature-dependent and, thus, become quenched at sufficiently low temperature.[24,25] Suppression of inhomogeneous broadening may be anticipated if the waveguide films contain a high degree of order on the PPWG surface. A microscopic characterization of the Tris films shows that it consists largely of flat, elongated microcrystals for dropcast films and small, rocklike crystals for sublimated films, that are randomly oriented

TABLE 1: Line-Center Frequencies and fwhm Linewidths (within parentheses) for the Tris Pellet and Tris Film Samples[a]

pellet[b]		dropcast film[b]		sublimated film[b]	
295 K	13 K	295 K	13.6 K	295 K	13.6 K
1.23[w]	1.31[w]		1.308 (0.021)		
					1.629 (0.015)
1.45 (0.21)	1.57 (0.16)	1.50 (0.07)	1.655 (0.017)	1.51 (0.07)	1.647 (0.012)
1.75[w]	1.76 (0.15)	1.78 (0.12)	1.706 (0.023)	1.80 (0.14)	1.701 (0.020)
					1.918 (0.165)
			2.064[w]		
			2.142 (0.027)		2.173 (0.039)
			2.181[sh]		2.246[w]
2.11(0.21)		2.22 (0.21)	2.393 (0.039)	2.14 (0.18)	2.392 (0.025)
			2.489 (0.040)		2.484[sh]
			2.691 (0.027)		2.712 (0.039)
	3.14[w]		3.176 (0.026)		3.177 (0.031)
			3.465[w]		3.471 (0.033)
			3.640 (0.083)		

[a] All values are in terahertz. [b] "w" represents a weak absorption line; "sh" represents a shoulder.

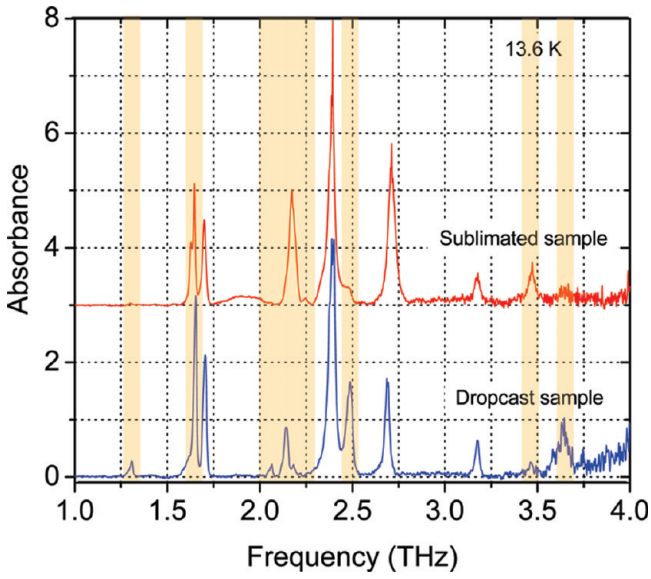

Figure 7. Comparison of the absorbance of dropcast and sublimated Tris thin films within a polished aluminum PPWG at 13.6 K. The colored bands indicate the difference between the two absorbance spectra.

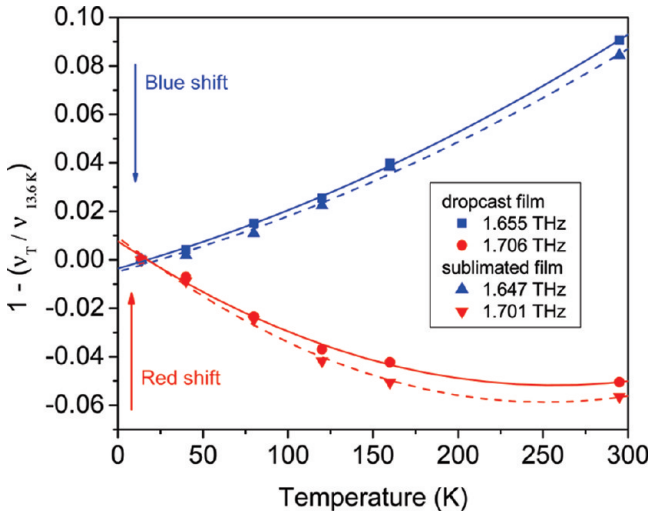

Figure 8. The temperature-dependent frequency shift for two vibrational modes of Tris dropcast and sublimated films. The y values are plotted as the fractional shift of the line frequency, υ_T, at temperature, T, from the line frequency, $\upsilon_{13.6K}$, measured at 13.6 K. The mode frequencies in the legend are the values measured at 13.6 K. The solid (dropcast film) and dashed lines (sublimated film) are quadratic fits to the data points.

on the PPWG surface but exhibit significant planar order with respect to the surface, as shown in Figure 2.

Figures 5 and 6 show that spectral features experience different frequency shifts upon cooling to 13.6 K. The features beyond 1.704 THz experience very negligible frequency shift. For the two specific resonances at 1.656 and 1.704 THz (at 13.6 K), the frequency shift is large but of a different sign. The resonance at 1.656 THz is seen to blue-shift from its room temperature value of 1.50 THz, and the one at 1.704 THz undergoes a red shift from 1.78 THz. This opposite shift of these two adjacent resonances is clearly observable in Figures 5 and 6. The fractional shift in frequency of these two resonances for dropcast as well as sublimated films is summarized in Figure 8. This fractional shift for 1.656 THz (blue shift) and 1.704 THz (red shift) is seen to follow a quadratic dependence with change in temperature.

In previous work,[10,12] Tris has been shown to crystallize in the orthorhombic system having $Pn2_1a$ space group with four molecules per unit cell. Tris crystallizes in a layered structure with strong hydrogen bonding within each layer and weak hydrogen bonds between layers. The blue frequency shift is, in part, due to compression of the crystalline lattice upon cooling, which results in a steeper intermolecular potential. Anharmonicity of the vibrational modes may also contribute to the shift.[26] The anomalous red shifting with cooling temperatures has been reported for some hydrogen bonding solids and has been interpreted to be due to weak intermolecular forces (van der Waals forces) that soften the vibrational potential as the temperature is lowered.[27,28] The extensive hydrogen bonding within the crystal lattice with differential hydrogen bonding strengths within the plane compared to between planes is considered to play a role in the red shift of resonances.[27,28]

Conclusion

Using waveguide THz-TDS we have obtained high resolution, narrow-line, high-sensitivity spectral measurements of the vibrational modes of Tris with resonances as narrow as 12 GHz in a spectral range from 100 GHz to 4 THz. The measurements reveal an impressive 12 observed lines for the dropcast film and 11 for the sublimated film at 13.6 K. The two films exhibit some different absorption features at 13.6 K, which indicates differential crystal ordering and orientation during the formation of the films. The line-narrowing effect observed for the waveguide films is related to the formation of microcrystals with high crystalline quality. These measurements are the first characterization of the far-infrared active vibrational mode frequencies of Tris in the terahertz (far-infrared) frequency range. At present, there are no theoretical predictions to compare with these observations. Clearly, these measurements provide strong experimental constraints on future theoretical modeling of the intermolecular and intramolecular structure of Tris.

Acknowledgment. The authors thank Joseph S. Melinger for useful discussion and comments on the manuscript. This work was supported in part by the National Science Foundation.

References and Notes

(1) Gomori, G. Buffers in the range of pH 6.5 to 9.6. *Proc. Soc. Exptl. Biol. Med.* **1946**, *62*, 33–34.

(2) Bates, R. G.; Robinson, R. A. Tris(hydroxymethy1)aminomethane—A useful secondary pH standard. *Anal. Chem.* **1973**, *45*, 420.

(3) Sirieix, D.; Deleyance, S.; Paris, M.; Massonnet-Castel, S.; Carpenter, A.; Baron, J. F. Tris(hydroxymethyl)aminomethane and sodium bicarbonate to buffer metabolic acidosis in an isolated heart model. *Am. J. Respir. Crit. Care Med.* **1997**, *155*, 957–963.

(4) Kallet, R. H.; Jasmer, R. M.; Luce, J. M.; Lin, L. H.; Marks, J. D. The treatment of acidosis in acute lung injury with Tris(hydroxymethyl)aminomethane. *Am. J. Respir. Crit. Care Med.* **2000**, *161*, 1149–1153.

(5) Swim, H. E.; Parker, R. F. Non-bicarbonate buffers in cell culture media. *Science* **1955**, *122*, 466.

(6) Mauler, H. R. The use of amine buffers in studies with enzymes. *Ann. N.Y. Acad. Sci.* **1961**, *92*, 426–440.

(7) Swim, H. E. Amine and other nonbicarbonate buffers in cell culture media. *Ann. N.Y. Acad. Sci.* **1961**, *92*, 440–446.

(8) Ramette, R. W.; Culberson, C. H.; Bates, R. G. Acid-base properties of tris(hydroxymethy1)aminomethane (Tris) buffers in seawater from 5 to 40 °C. *Anal. Chem.* **1977**, *49*, 867.

(9) Wilson, W. A.; Clark, M. T.; Pellmar, T. C. Tris buffer attenuates acetylcholine responses in aplysia neurons. *Science* **1977**, *196*, 440–441.

(10) Rudman, R.; Eilerman, D. The structure of crystalline Tris: A plastic crystal precursor, buffer, and acetylcholine attenuator. *Science* **1978**, *200*, 531–533.

(11) Nahas, G. G. The pharmacology of tris(hydroxymethyl)aminomethane (THAM). *Pharm. Rev.* **1962**, *14*, 447–472.

(12) Eilerman, D.; Rudman, R. Polymorphism of crystalline poly(hydroxymethyl) compounds. III. The structures of crystalline and plastic tris(hydroxymethyl)aminomethane. *J. Chem. Phys.* **1980**, *72*, 5656.

(13) Divi, S.; Chellappa, R.; Chandra, D. Heat capacity measurement of organic thermal energy storage materials. *J. Chem. Thermodyn.* **2006**, *38*, 1312–1326.

(14) Schroetter, S.; Bougeard, D. The calculated and observed vibrational spectra of the ordered phase of tris(hydroxymethyl)aminomethane. *Ber. Bunsenges. Phys. Chem.* **1987**, *91*, 1271.

(15) Kanesaka, I.; Mizuguchi, K. Vibrational study of hydrogen bonds and structure of Tris(hydroxymethyl)aminomethane. *J. Raman. Spectrosc.* **1998**, *29*, 813–817.

(16) Brandt, N. N.; Chikishev, A. Y.; Sakodinskaya, I. K. Raman spectroscopy of tris(hydroxymethyl)aminomethane as a model system for studies of α-chymotrypsin activation by crown ether in organic solvents. *J. Mol. Struct.* **2003**, *648*, 177–182.

(17) Zhang, J.; Grischkowsky, D. Waveguide THz time-domain spectroscopy of nm water layers. *Opt. Lett.* **2004**, *19*, 1617–1619.

(18) Melinger, J. S.; Laman, N.; Harsha, S. S.; Grischkowsky, D. Line narrowing of terahertz vibrational modes for organic thin polycrystalline films within a parallel plate waveguide. *Appl. Phys. Lett.* **2006**, *89*, 251110.

(19) Melinger, J. S.; Laman, N.; Harsha, S. S.; Grischkowsky, D. High-resolution waveguide terahertz spectroscopy of partially oriented organic polycrystalline films. *J. Phys. Chem. A* **2007**, *111*, 10977.

(20) Grischkowsky, D.; Keiding, S.; van Exter, M.; Fattinger, C. Far-infrared time-domain spectroscopy with terahertz beams of dielectrics and semiconductors. *J. Opt. Soc. Am. B* **1990**, *7*, 2006–2015.

(21) van Exter, M.; Grischkowsky, D. Characterization of an optoelectronic terahertz beam system. *IEEE Trans. Microwave Theory Tech.* **1990**, *38*, 1684–1691.

(22) Mendis, R.; Grischkowsky, D. Undistorted guided wave propagation of sub-picosecond THz pulses. *Opt. Lett.* **2001**, *26*, 846–848.

(23) Harsha, S.; Laman, N.; Grischkowsky, D. High Q terahertz Bragg resonances within a metal parallel plate waveguide. *Appl. Phys. Lett.* **2009**, *94*, 091118.

(24) Hess, L. A.; Prasad, P. N. Vibrational dephasing in organic solids: Temperature dependence of a Raman active localized internal mode of naphthalene. *J. Chem. Phys.* **1980**, *72*, 573–579.

(25) Dlott, D. D. Optical phonon dynamics in molecular crystals. *Annu. Rev. Phys. Chem.* **1986**, *37*, 157.

(26) Ouillon, R.; Ranson, P.; Califano, S. Temperature dependence of the bandwidths and frequencies of some anthracene phonons. High resolution Raman measurements, *Chem. Phys.* **1984**, *91*, 119–131.

(27) Walther, M.; Fischer, B. M.; Jepsen, P. U. Noncovalent intermolecular forces in polycrystalline and amorphous saccharides in the far infrared. *Chem. Phys.* **2003**, *288*, 261.

(28) Fischer, B. M.; Helm, H.; Jepsen, P. U. Chemical recognition with broadband THz spectroscopy. *Proc. IEEE* **2007**, *95*, 1592–1604.

JP911135U